A Tunable Photo-Electric co-Excited Point Electron Source: Low-Intensity Excitation Emitting and Structure-Modulated Spectrum-Selecting

Yinyao Chen,[a] Shuai Tang,[a] Yan Shen,*[a] Huanjun Chen,[a] and Shaozhi Deng [a]

[a] State Key Laboratory of Optoelectronic Materials and Technologies, Guangdong Province Key Laboratory of Display Material and Technology, School of Electronics and Information Technology, Sun Yat-sen University, Guangzhou 510275, China
*E-mail: shenyan7@mail.sysu.edu.cn

Supporting Information I: Emission current stability, field enhancement factor and emitting area calculations

Figure S1 gives an emission current stability measurement of the W needle nano-cold-cathode as a point electron source for a duration of 540 s. The electron emission stability is characterized by calculating the actual current fluctuation, which is expressed as $\langle \Delta I^2 \rangle^{1/2}/\langle I \rangle$ (in which $\langle I \rangle$ is the average current and $\Delta I = I - \langle I \rangle$ is the deviation of current from its average value). From Figure S1, one can conclude that when the emission current of the W needle cathode is 7.26 nA and 3.65 nA, the corresponding current fluctuation values is 3.57% and 5.32%, respectively, under a fixed biased electric field of 0.425 and 0.398 V μm^{-1}. We therefore believe that under such a low vacuum condition of 10^{-6} Pa, the electron emission stability of the W point electron source cathode developed by us is good at nA level, which is quite stable compared with that for the commercial W(310) emitter[S1] at ~1×10^{-7} Pa.

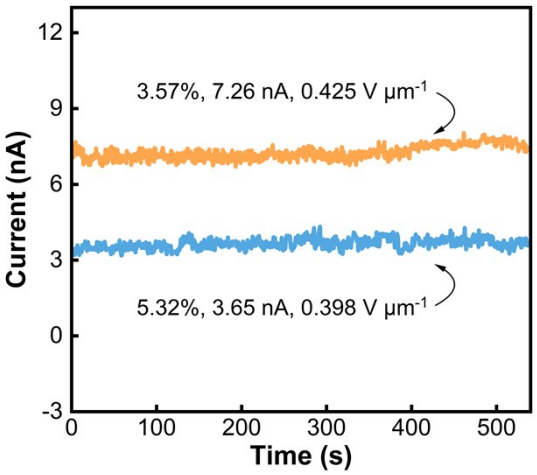

Fig. S1 The 540 s stability of a W needle nano-cold-cathode point electron source, at fixed biased electric field of 0.425 and 0.398 V μm^{-1}, respectively.

The photo-electric co-excited electron emission properties of the tungsten (W) needle nano-cold-cathode were measured in a vacuum chamber (~1 × 10^{-6} Pa). Figure 1c in the main text shows the field emission current *versus* biased electric field (I-E_{bias}) curve (see the blue plots), which was extracted to transform the corresponding Fowler-Nordheim (F-N) plots (inset in Figure 1c) for further field enhancement factor and emitting area calculations. The linear F-N relation between ln(I/E^2) and 1/E corresponding to Equation 1 is:[S2-4]

$$\ln\frac{I}{E^2} = \frac{k}{E} + b \qquad \text{(S1)}$$

where the slope $k = -s_t B\phi^{3/2}/\beta$ and the intercept $b = \ln(AS\beta^2 r_y/\phi)$, s_t and r_y are the appropriate correction function values of the slope and the intercept, respectively, whose expressions are:

$$s_t = 1 - \frac{1}{6}y^2 \tag{S2}$$

$$r_y = \left(1 + \frac{1}{9}y^2\left[1 - \ln y\right]\right)^{-2} e^{9.836\left(\frac{5}{6} - \frac{1}{3}\ln y\right)\Big/\phi^{1/2}} \tag{S3}$$

where $y = 3.79e^{-5}E^{1/2}/\phi$. The expressions for the appropriate specific values of v_y and tangential energy d (in eV) for the current correction function appearing in the text are as follows:[S3-5]

$$v_y = 1 - y^2 + \frac{1}{3}y^2 \ln y \tag{S4}$$

$$d = 9.76 \times 10^{-11} \frac{E}{\phi^{1/2} t_y} \tag{S5}$$

where t_y is the image potential correction factor, with expression as follows:[S6]

$$t_y = 1 + 0.1107 y^{1.33} \tag{S6}$$

By fitting the F-N curve when laser was off, it shows a very good linear distribution (with fitness $R^2 = 0.999$). According to eqn S1, it can be derived that its slope $k = -6.6075$ and intercept $b = -3.705$. Assuming that the work function ϕ of W is 4.5 eV, a numerical calculation combined with eqn S1-S6 yields a field enhancement factor $\beta \approx 9.68 \times 10^3$, while the emitting area of the W needle $S \approx 8$ nm^2.

Supporting Information II. Collected current *versus* cathode decelerating voltage curves with respect to vacuum energy level in the electron energy spread (ΔE) measurement, which were extracted under five different laser-intensity excitations of supercontinuum white-light laser.

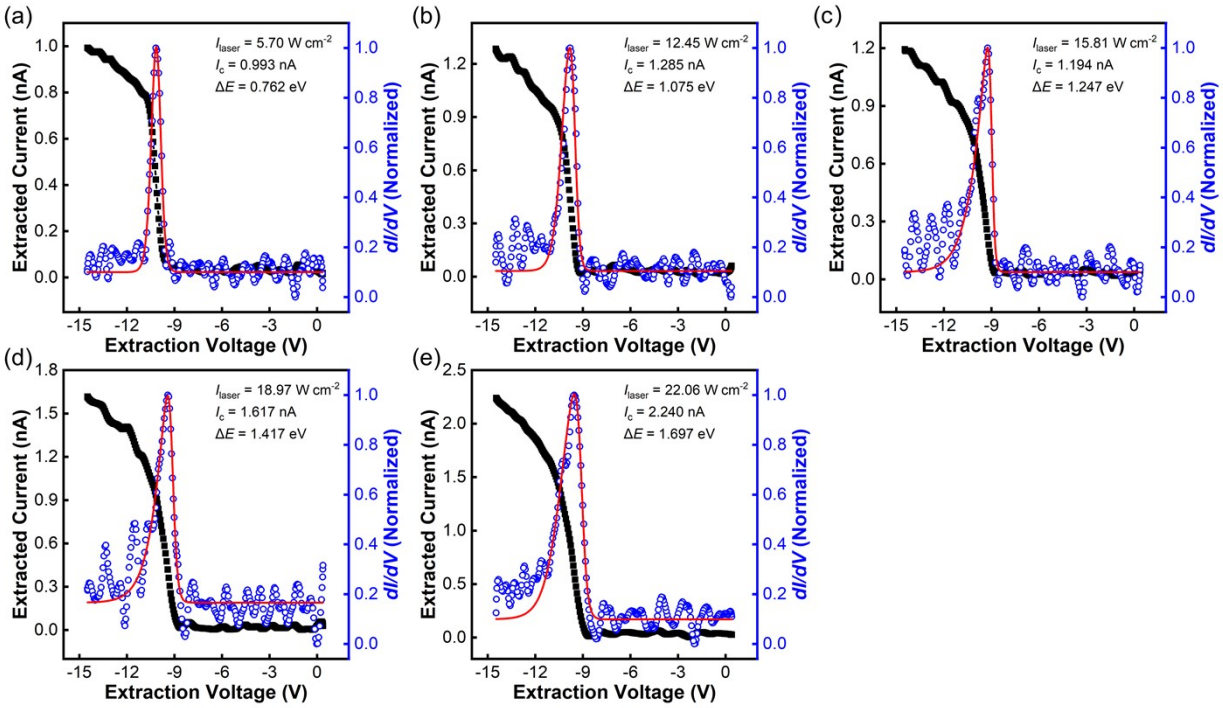

Fig. S2 The relationship between the cathode decelerating voltages and the collected currents relative to the vacuum energy level, under different laser-intensity white-light excitations (I_{laser}) of (a) 5.70 W cm^{-2}, (b) 12.45 W cm^{-2}, (c) 15.81 W cm^{-2}, (d) 18.97 W cm^{-2}, and (e) 22.06 W cm^{-2}, respectively. The biased electric field (E_{bias}) was fixed at 0.318 V μm^{-1}. By differentiating the experimentally recorded integral spectrum (see the black dotted lines), the electron energy spreads (see the blue scatter patterns) could be obtained, and the full width at half maximum (FWHM) of each single-peak fitting curve was represented as the symbol ΔE.

Supporting Information III. The dependence relationship between the emission current and laser-intensity under different excitation bands.

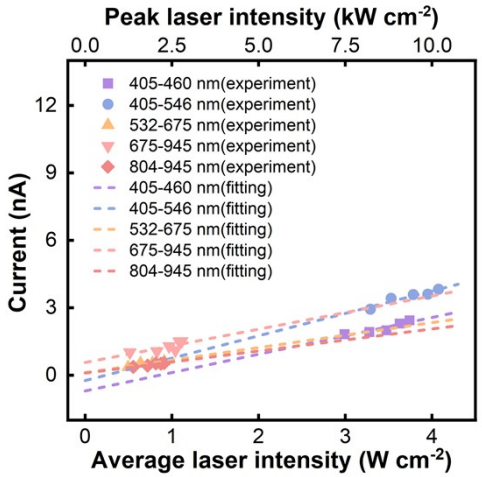

Fig. S3 The dependence of the emission current (I) on I_{laser} under different excitation frequency-bands. The E_{bias} was fixed to 0.45 V μm^{-1}, and the excitation bands were selected as 405-460 nm (with CWL of ~432.5 nm), 405-546 nm (CWL~475.5 nm), 532-675 nm (CWL~603.5 nm), 675-945 nm (CWL~810 nm), and 804-945 nm (CWL~874.5 nm), respectively. Herein, the scatters are the experimental data and the dotted lines are their corresponding linear fitting data.

Supporting Information Ⅳ. The influence of geometric parameters of W needle nano-cold-cathode on the light absorption under different polarization directions.

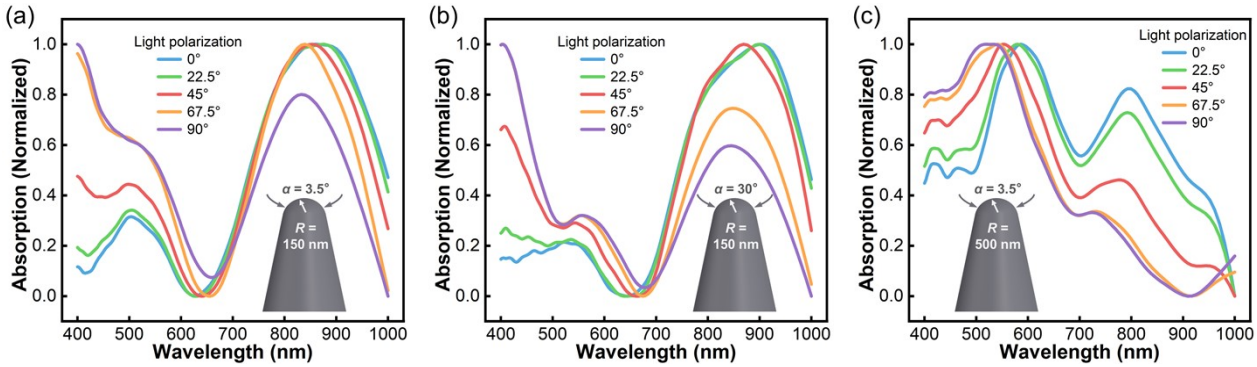

Fig. S4 The absorption of incident light on the W needle structure with different geometric features under different polarizations (represented by the normalized absorption spectrum). The tip curvature radius and cone angle are set to (a) *R*~150 nm, α~3.5°, (b) *R*~150 nm, α~30°, (c) *R* ~500 nm, α~3.5°, respectively. Inset: Schematic diagram of the corresponding geometric model.

Supporting Information V. Controllable fabrication of the W needle nano-cold cathodes with different geometric features. The geometric characteristic parameters such as *R* and α were effectively adjusted by the fabricating process steps of electro-chemical etching.

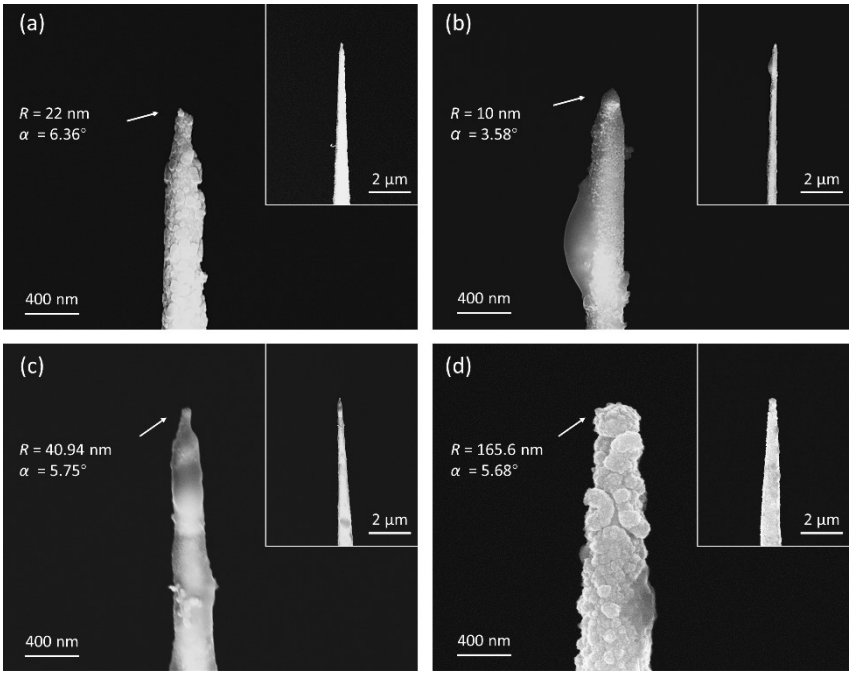

Fig. S5 SEM morphologies of the W needles fabricated with different electro-chemical etching conditions. The tip curvature radius (*R*) and cone angle (α) of the needle samples are as follows: (a) *R*~22 nm, α~6.36°, (b) *R*~10 nm, α~3.58°, (c) *R*~ 40.94 nm, α~ 5.75°, (d) *R*~ 165.6 nm, α~5.68. Insets: The corresponding low-magnification SEM images.

Table S1. Comparison between the fabricating-process parameters of the W needle nano-cold-cathode and the corresponding geometric features of the produced structure.

Sample No.	Supply voltage (V)	Etching potential (V)	Etching current (mA)	Immersed length (μm)	R (nm)	α (°)
1	12	3	9	244	126.55	6.66
2	12	1.55	16	269	22	6.36
3	12	1.72	15	373	10	3.58
4	12	1.25	18	338	40.94	5.75
5	12	0.9	14	270	165.6	5.68

Note: The diameter of W wire was 0.2 mm. The concentration of electrolyte solution was 2 mol L^{-1}. The etching initiation current could reflect the change of the immersed length, and the higher the initiation current, the longer the immersed length. Simply pursuing the sharpness of W needle would result in excessive length and imbalance aspect ratio, leading to a decrease in emitter quality. Therefore, it is necessary to balance all aspects well. The sample presented in Figure 1a in the main text is Sample No. 1 after DC heating and cleaning.

References

S1 H. Zhang, J. Tang, J. Yuan, Y. Yamauchi, T. T. Suzuki, N. Shinya, K. Nakajima and L. C. Qin, *Nat Nanotechnol*, 2016, **11**, 273-279.
S2 R. G. Forbes, *Rev Sci Instrum*, 2020, **91**, 107101.
S3 S. Tang, J. Tang, Y. Wu, Y. H. Chen, J. Uzuhashi, T. Ohkubo and L. C. Qin, *Nanoscale*, 2021, **13**, 17156-17161.
S4 E. L. Murphy and R. H. Good, *Phys Rev*, 1956, **102**, 1464-1473.
S5 R. G. Forbes, *Appl Phys Lett*, 2006, **89**, 113122.
S6 S. Tang, J. Tang, T.-w. Chiu, W. Hayami, J. Uzuhashi, T. Ohkubo, F. Uesugi, M. Takeguchi, M. Mitome and L.-C. Qin, *Nano Res*, 2020, **13**, 1620-1626.